Supplementary Information (SI) for Nanoscale.

Regulating Sodium Storage Sites in Carbon Materials via Fluorine doping for Sodium Ion Batteries

Zhiqiang Li[a,b,c], Jiayao Yu*[b,c], Ge Yao[b], Fangcai Zheng*[b,c]

[a]School of Energy Materials and Chemical Engineering, Hefei University, Hefei, Anhui, 230031, P. R. China

[b]Institutes of Physical Science and Information Technology and School of Materials Science and Engineering, Anhui University, Hefei, 230601, P. R. China

[c]High Magnetic Field Laboratory, Hefei Institutes of Physical Science, Chinese Academy of Sciences, Hefei, Anhui, 230031, P. R. China

*Corresponding authors: zfcai@mail.ustc.edu.cn (F.C. Zheng)

jiayaoyu@stu.ahu.edu.cn (J.Y. Yu)

Experimental section

1. Materials synthesis

1.1 Materisls

Zinc nitrate hexahydrate ($Zn(NO_3)_2·6H_2O$), 2,3,5,6-tetrafluoroteraphethalic acid (H_2TFBDC), 1,4-dicarboxybenzene (BDC), Methanol (CH_3OH), nitric acid (HNO_3). All chemicals were used as received without further purification.

1.2 Synthesis of fluorine-doped carbon nanorods (FCNs)

The Zn-TFBDC was synthesized by a simple solvothermal method. $Zn(NO_3)_2·6H_2O$ (2.41 g) and H_2TFBDC (0.72 g) were successively added to anhydrous ethanol (50 ml) and dissolved by ultrasonication for 15 min to achieve a homogeneous mixed solution. The mixed solution was transferred into a 100 ml Teflon-lined stainless autoclave, and maintained at 120 °C for 12 h. The product was collected by centrifugation, washed with anhydrous ethanol for three times, and dried at 60 ℃ overnight. The as-prepared precursor was annealed at 600 °C for 2 h under vacuum conditions with a heating rate of 10 °C min^{-1} and then etched in 3 M HNO_3 for 12 h. The etched samples were centrifuged, washed, collected, and dried overnight at 60 °C. The corresponding samples were denoted as FCNs. Additionally, the synthesis methods for FCNs-500 and FCNs-700 are essentially identical to those for FCNs, with only the carbonization temperatures adjusted to 500 °C and 700 °C, respectively. For the synthesis of NCs, only the precursor preparation process involves replacing H_2TFBDC with BDC.

2. Materials characterization

The crystal structures of all samples were determined with an X-ray diffractometer (Rigaku Co, Japan, D/MAX-γA) with Cu-Kα radiation (λ=0.154 nm). The morphologies of the as-prepared samples were investigated using scanning electron microscopy (SEM, JEOL JSM-6700 M) with a voltage of 200 kV and transmission electron microscopy (TEM, Hitachi H-800) using an accelerating voltage of 200 kV. High resolution transmission electron microscopy (HRTEM, JEOL-2011) was further performed to investigate the structure. The electronic states of all elements in samples were investigated by X-ray photoelectron spectroscopy (XPS, ESCALAB 250). The

Raman spectrum was obtained using a Confocal Laser MicroRaman Spectrometer (Via-Reflex/inVia-Reflex). The specific surface area and pore structure were measured by using a sorption analyzer (Micromeritics ASAP 2020) at 77 K.

3. Electrochemical measurements

All the electrochemical measurements were characterized employing half coin cells (CR2032) assembled in an argon-filled glove box with the concentrations of oxygen and moisture below 1 ppm (MBRAUN UNILAB PRO, SP (1800/780)). The as-prepared sample (80%), polyvinylidene difluoride (PVDF, 10%), and carbon black (10%) were mixed in N-methylpyrrolidone (NMP), to obtained the homogeneous slurry for the working electrodes. Finally, the homogeneous slurry was coated on a copper current collector and dried at 80 °C overnight under vacuum conditions. The mass loading of the electrode materials is about 0.6-0.7 mg. The glass fiber (GF/D, Whatman) was used as the separator. The metallic Na was used as the counter electrode. The electrolyte was 1 M $NaPF_6$ in ethylene carbonate and diethyl carbonate (EC : DEC = 1 : 1) with 5% fluoroethylene carbonate (FEC). The galvanostatic charge-discharge tests was measured by the Neware CT3008 W instrument within a voltage window of 0.01−3.0 V. Cyclic voltammetry (CV) and electrochemical impedance spectroscopy (EIS) were performed on CHI760E electrochemical workstation.

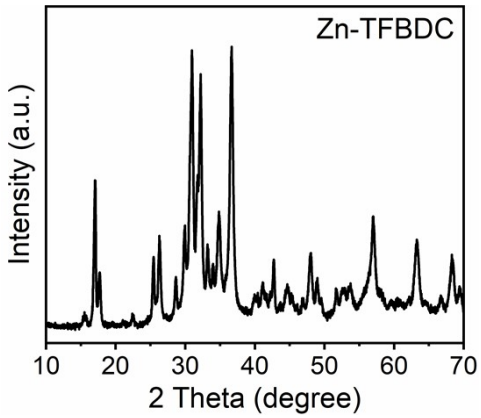

Fig. S1. XRD pattern of as-prepared Zn-TFBDC.

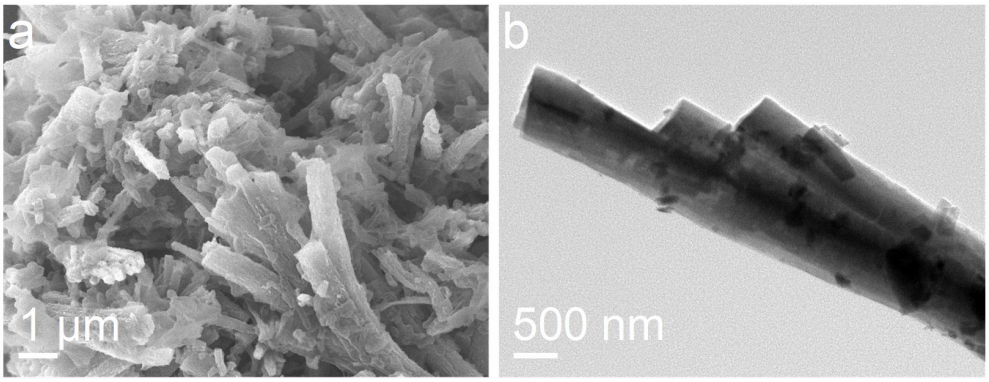

Fig. S2. (a) SEM and (b) TEM images of Zn-TFBDC.

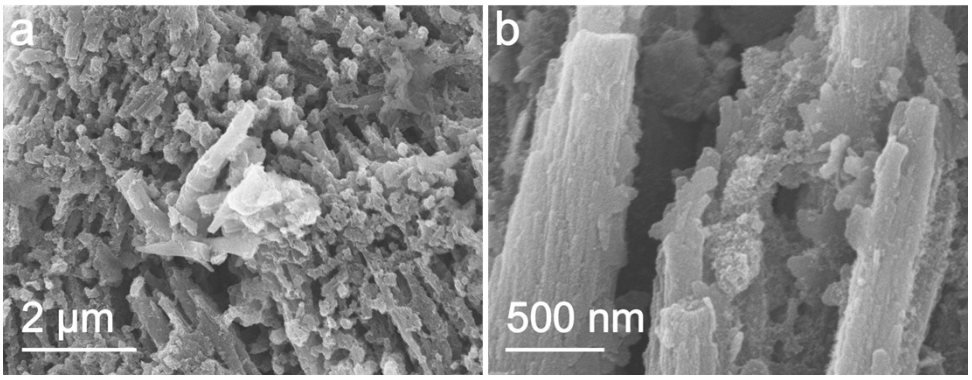

Fig. S3. SEM images of FCNs.

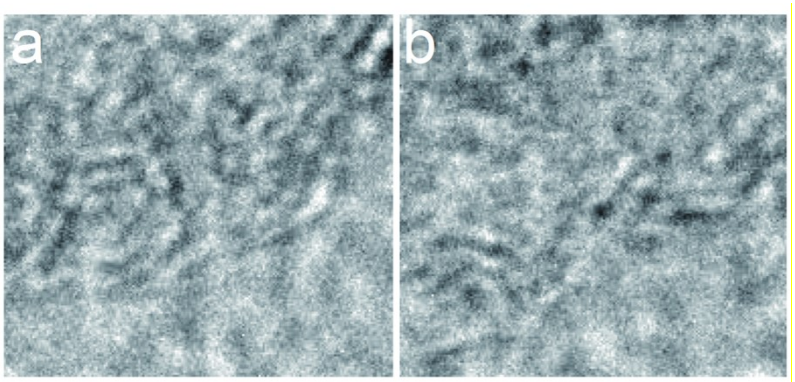

Fig. S4. Edge defects in FCNs.

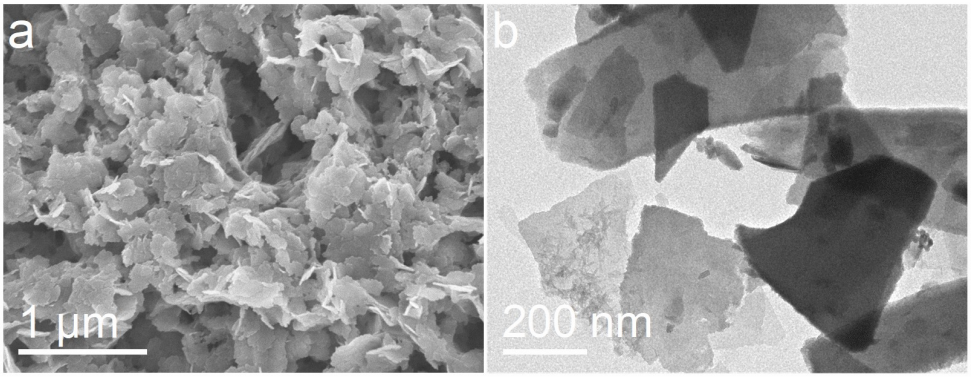

Fig. S5. (a) SEM and (b) TEM images of CNs.

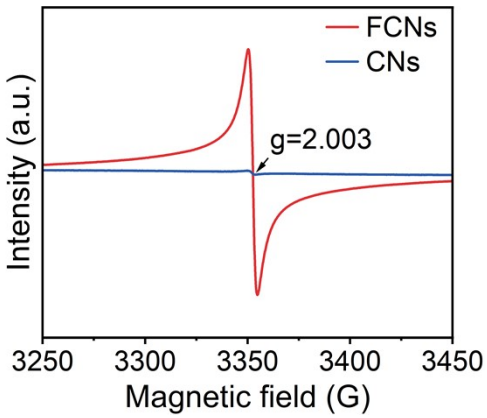

Fig. S6. EPR spectra of FCNs and CNs.

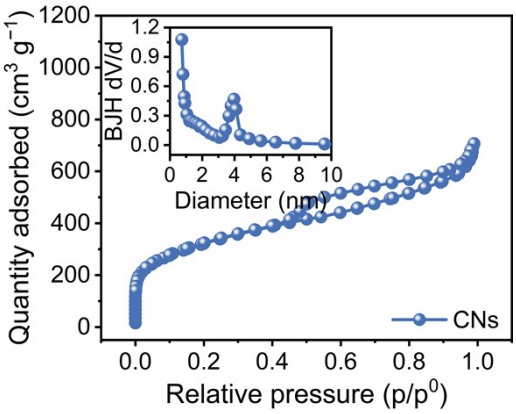

Fig. S7. N_2 adsorption/desorption isotherms of CNs, insert is corresponding pore size distributions.

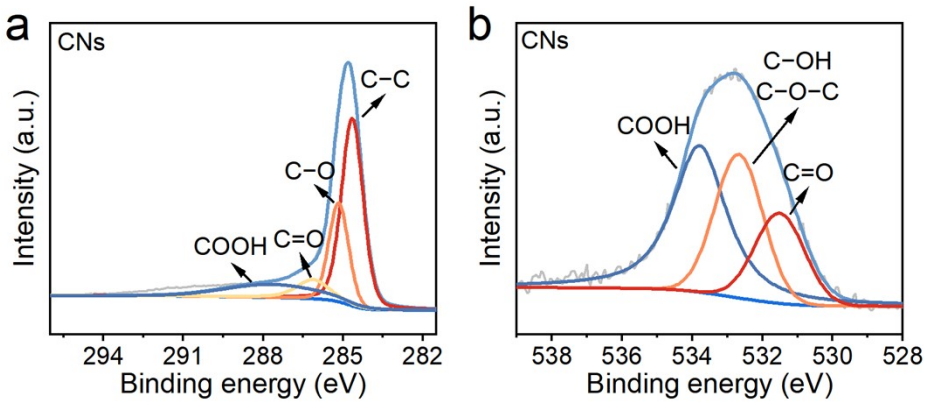

Fig. S8. The high-resolution XPS spectra of (a) C 1s, (b) O 1s for the CNs.

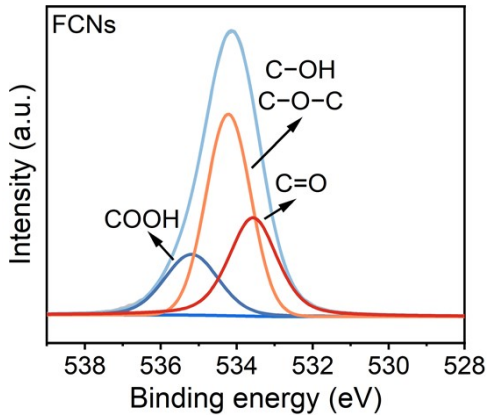

Fig. S9. The high-resolution XPS spectrum of O 1s for the FCNs.

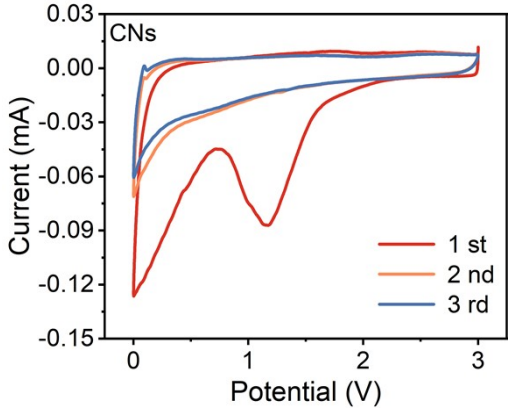

Fig. S10. CV curves of CNs at 0.1 mV s^{-1}.

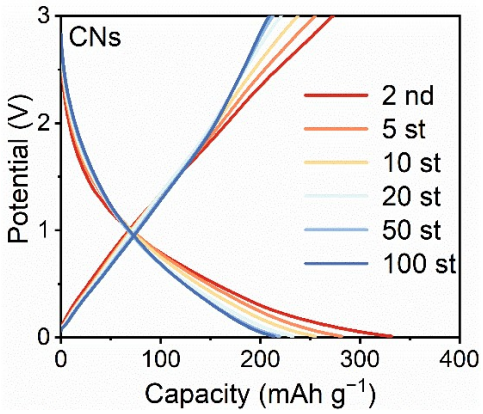

Fig. S11. GCD curves of CNs.

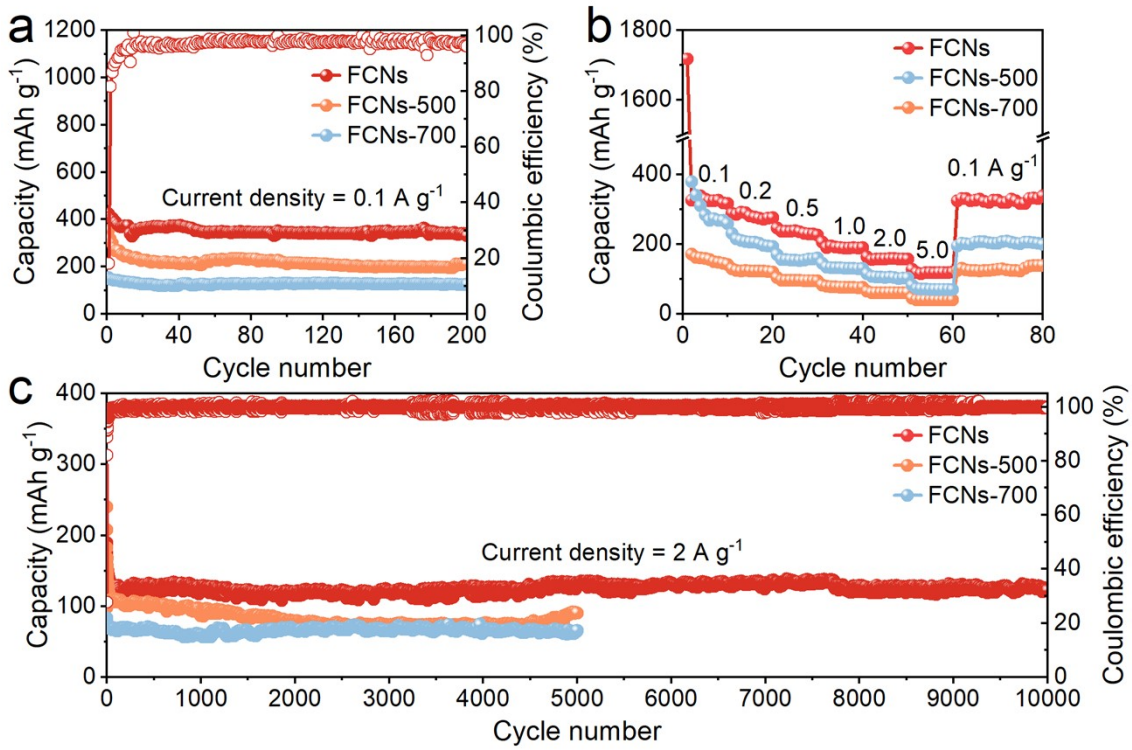

Fig. S12. (a) cycling performance and (b) rate capability of FCNs at different anneal temperature. (e) Long-term cycling stability at 2 A g^{-1}.

The FCNs-500 and FCNs-700 were prepared at the same reaction steps except that the carbonization temperatures were set at 500 and 700 °C, respectively.

From Fig. S12, the FCNs has the best electrochemical performance, demonstrate that the best carbonization temperatures is 600 ℃.

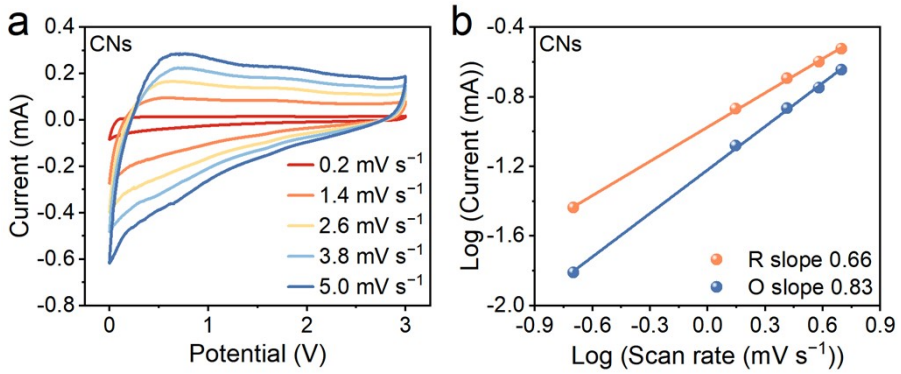

Fig. S13. (a) CV curves of CNs at different scan rates in the range of 0.2 to 5.0 mV s^{-1}. (b) The b slope value of CNs.

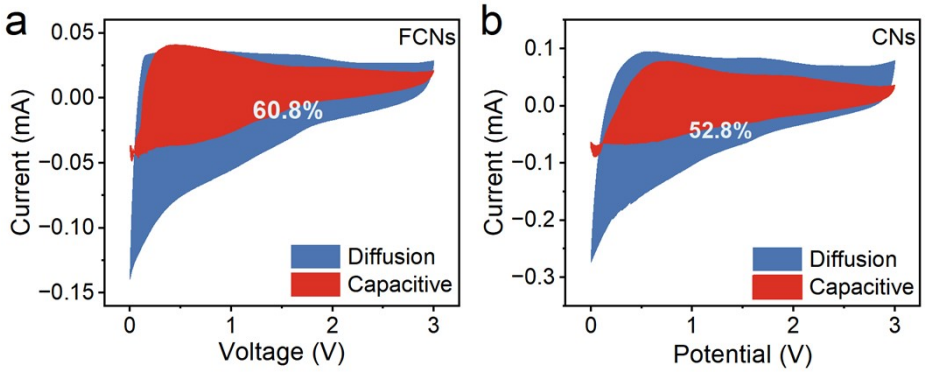

Fig. S14. Capacitive charge storage contribution ratios of FCNs and CNs at scan rates of 1.4 mV s^{-1}.

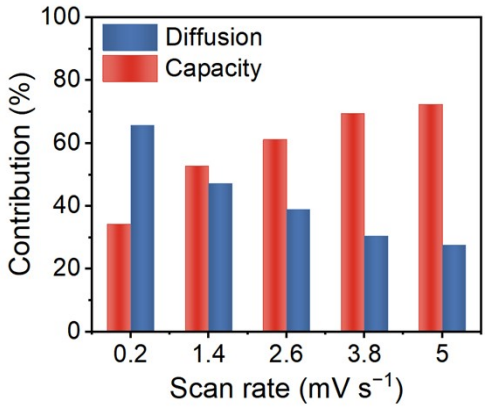

Fig. S15. Contribution ratio of the capacitive process in CNs at different scan rates.

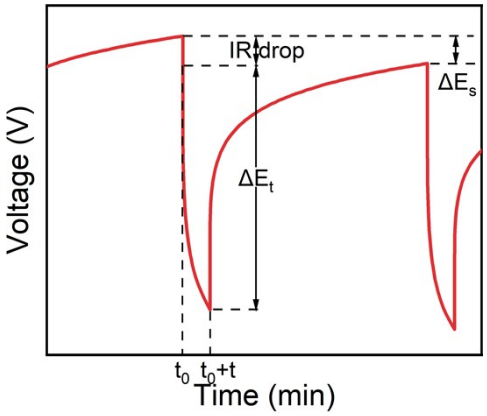

Fig. S16. Schematic of the calculation of diffusion coefficient using the GITT technique.

The diffusion coefficient is calculated according to the equation:[S1]

$$D = \frac{4}{\pi\tau}\left(\frac{m_b V_m}{M_B S}\right)^2\left(\frac{\Delta E_S}{\Delta E_t}\right)^2$$

Where τ is the current pulse time (s), m_B, M_B, and V_M are the mass, the molar mass and the molar volume of the active material, respectively. S is the geometric area of the electrode.

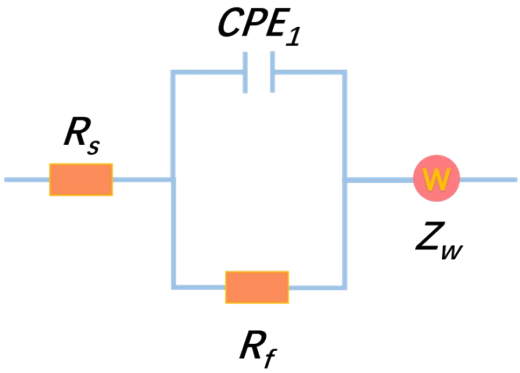

Figure S17. The equivalent circuit model of EIS.

Table S1. The N_2 adsorption/desorption isotherms results of all electrode materials.

Sample	Specific surface area ($m^2\ g^{-1}$)	Pore volume ($cm^3\ g^{-1}$)	Pore diameter (nm)
FCNs	579.7	1.19	8.19
CNs	1156.6	1.10	3.79

Table S2. Comparison of electrochemical performance of FCNs electrode with those previous reported carbon-based materials for SIBs.

Materials	Current density ($A\ g^{-1}$)	Cycle number	Capacity ($mAh\ g^{-1}$)	Reference
SBNC	0.05	500	308	S2
CSSHC-1300	0.03	200	270	S3
GLC-900	0.1	1000	~200	S4
2	0.1	800	290.6	S5
NS-HCS	0.1	100	274.8	S6
CHC-0.25	0.05	50	319.5	S7
S-CBC	0.1	50	302.9	S8
SC-5.00	0.1	500	184.7	S9
OSHC-Air	0.05	100	320	S10
NHC-2	0.3	100	238.24	S11
FCNs	0.1	200	331	This work

Table S3. The Na adsorption energy of all electrode materials.

Sample	FCNs	CNs
adsorption energy	3.38	2.06

Reference:

S1 J. Yang, G. Yao, Z. Li, Y. Zhang, L. Wei, H. Niu, Q. Chen and F. Zheng, *Small*, 2023, **19**, 2205544

S2 Y. Tang, X. Wang, J. Chen, D. Wang and Z. Mao, *Chem. Eng. J.*, 2022, **427**, 131951.

S3 J. Peng, H. Tan, Y. Tang, J. Yang, P. Liu, J. Liu, K. Zhou, P. Zeng, L. He and X. Wang, *J. Energy Storage*, 2024, **101**, 113864.

S4 H.-J. Li, S.-P. Shen, G. Tang, J.-J. Li, X.-F. Lyu, L.-J. Zhu, F. Jiang, Y.-Q. Chen, J. Yue and Z. Chen, *Electrochim. Acta*, 2022, **419**, 140423.

S5 N. Ahmad, N. Muhammad, H. Chen, J. Wang, C. Wei, M. Khan and R. Yang, *J. Colloid Interface Sci.*, 2023, **650**, 1725-1735.

S6 D. Sun, S. Lin, D. Yu, Z. Wang, F. Deng, X. Zhou, G. Ma and Z. Lei, *Chin. Chem. Lett.*, 2023, **34**, 107339.

S7 S. Guo, Y. Chen, L. Tong, Y. Cao, H. Jiao, Z. long and X. Qiu, *Electrochim. Acta*, 2022, **410**, 140017.

S8 X. Wang, X. Xiao, C. Chen, B. Sun, X. Chen, J. Hu, L. Zhang and D. Sun, *Dalton Trans.*, 2023, **52**, 12253-12263.

S9 J. Miralda-Jalle, J. E. Haskouri, M. M. Leite, T. Kennedy, M. Culebras and M. N. Collins, *Bioresour. Technol.*, 2025, **428**, 132468.

S10 L. Zhou, Y. Cui, P. Niu, L. Ge, R. Zheng, S. Liang and W. Xing, *Carbon*, 2025, 231, 119733.

S11 D. Wang, L. Feng, D. Mo, Y. Zhang, X. Zheng, G. Xie and X. Guo, *Inorg. Chem. Front.*, 2026, **13**, 310-318.